

Suppressed optical field and electron leakage and enhanced hole injection in InGaN laser diodes with InGaN–GaN–InGaN barriers

Cite as: J. Appl. Phys. **130**, 183104 (2021); <https://doi.org/10.1063/5.0071035>

Submitted: 10 September 2021 • Accepted: 21 October 2021 • Published Online: 11 November 2021

 Liwen Cheng, Jiayi Zhang, Jundi Wang, et al.



View Online



Export Citation



CrossMark

ARTICLES YOU MAY BE INTERESTED IN

[GaN-based power devices: Physics, reliability, and perspectives](#)

Journal of Applied Physics **130**, 181101 (2021); <https://doi.org/10.1063/5.0061354>

[Lasing below 170 nm using an oscillator FEL](#)

Journal of Applied Physics **130**, 183101 (2021); <https://doi.org/10.1063/5.0064942>

[2D Quantum materials: Magnetism and superconductivity](#)

Journal of Applied Physics **130**, 180401 (2021); <https://doi.org/10.1063/5.0075774>



Applied Physics
Reviews

Read. Cite. Publish. Repeat.

19.162

2020 IMPACT FACTOR*





Suppressed optical field and electron leakage and enhanced hole injection in InGaN laser diodes with InGaN–GaN–InGaN barriers

Cite as: J. Appl. Phys. **130**, 183104 (2021); doi: [10.1063/5.0071035](https://doi.org/10.1063/5.0071035)

Submitted: 10 September 2021 · Accepted: 21 October 2021 ·

Published Online: 11 November 2021



Liwen Cheng,^{1,a)}  Jiayi Zhang,¹ Jundi Wang,¹ Jun Zhang,² Jinpeng Yang,¹ Shudong Wu,¹ Qinyu Qian,¹  and Haitao Chen¹

AFFILIATIONS

¹College of Physical Science and Technology, Yangzhou University, Yangzhou 225002, China

²Changchun Institute of Optics, Fine Mechanics and Physics, Chinese Academy of Sciences, Changchun 130033, China

^{a)}Author to whom correspondence should be addressed: lwcheng@yzu.edu.cn

ABSTRACT

In this study, an InGaN laser diode (LD) with InGaN–GaN–InGaN quantum barriers was proposed and studied systematically. The energy band diagrams, stimulated recombination rate, optical field distribution, current distribution near the active region, and power–current–voltage performance curves were investigated. The simulation results suggest that the LD with InGaN–GaN–InGaN quantum barriers has better performance than the LD with conventional GaN and InGaN quantum barriers because of the properly adjusted refraction index profile and energy band diagrams, which are advantageous to both the suppressed leakage of the optical field and electrons out of and the enhanced injection of holes into the active region.

Published under an exclusive license by AIP Publishing. <https://doi.org/10.1063/5.0071035>

I. INTRODUCTION

InGaN-based laser diodes (LDs) have broad applications in diverse areas, for instance, mobile laser projectors, data storage, and photolithographic processes.^{1–3} Despite much progress having been made in this technology in the past two decades, better performance is expected for the application of LDs as a light source in more areas, such as solid-state lighting, full-color displays, and high density optical storage.^{4–6}

To improve the InGaN LDs performance, much investigation has been conducted on the epitaxy structure design and the physical mechanisms. Most work concentrates mainly on redesigning the electron-blocking layer (EBL)^{7–9} to impede electron leakage and optimize the waveguide layer^{10–12} or cladding layer (CL),^{13–15} which improves the optical confinement factor (OCF) in the active region and reduces the optical absorption loss (OAL) in the LDs. Relatively few studies of the multiple quantum well (MQW) active region have been made. A recent study reported that employing InGaN quantum barriers (QBs) with higher refractive indices to replace conventional GaN QBs can improve the optical confinement and, thus, the performance of these LDs.¹⁶ However, using

the InGaN as a QB will decrease the carrier confinement in the MQWs due to its smaller energy bandgap.

In this paper, a consideration of the advantages of the InGaN QBs and GaN QBs led to the proposal of an LD with InGaN–GaN–InGaN (IGI) QBs. Theoretical studies of the electrical and optical characteristics of the proposed LDs and LDs with InGaN QBs and GaN QBs are conducted using LASTIP software,¹⁷ which has been successfully applied to simulate realistic devices.^{9,12,16}

II. STRUCTURES AND PARAMETERS

The InGaN MQW LD with conventional GaN QBs used in the simulation is based on Ref. 18. The LD was composed of an n-type GaN ($3 \times 10^{18} \text{ cm}^{-3}$) substrate, an n-type $\text{Al}_{0.08}\text{Ga}_{0.92}\text{N}$ ($3 \times 10^{18} \text{ cm}^{-3}$) CL with a thickness of $1 \mu\text{m}$, an n-type GaN ($5 \times 10^{17} \text{ cm}^{-3}$) lower waveguide layer with a thickness of $0.12 \mu\text{m}$, and two 2.5 nm thickness $\text{In}_{0.15}\text{Ga}_{0.85}\text{N}$ QWs separated by three 14 nm thickness GaN QBs. Following is a p-type $\text{Al}_{0.15}\text{Ga}_{0.85}\text{N}$ ($5 \times 10^{19} \text{ cm}^{-3}$) EBL with a thickness of 20 nm , a p-type GaN ($2 \times 10^{19} \text{ cm}^{-3}$) upper waveguide layer with a thickness of $0.1 \mu\text{m}$, a p-type $\text{Al}_{0.06}\text{Ga}_{0.94}\text{N}$ ($2 \times 10^{19} \text{ cm}^{-3}$) CL with a thickness of $0.6 \mu\text{m}$,

and a p-type GaN ($1 \times 10^{20} \text{ cm}^{-3}$) ohmic contact layer with a thickness of 40 nm. The LDs with IGI QB structures are similar to the LD with GaN QBs, except that the conventional 14 nm GaN QB was divided into three parts, consisting of a 3.5 nm $\text{In}_{0.04}\text{Ga}_{0.96}\text{N}$, a 7 nm GaN, and a 3.5 nm $\text{In}_{0.04}\text{Ga}_{0.96}\text{N}$. In addition, for comparative analysis, another LD with $\text{In}_{0.02}\text{Ga}_{0.98}\text{N}$ QBs was also studied. The overall In content in the LDs with IGI and InGaN QBs is exactly the same. The cavity length for the three LDs was $600 \mu\text{m}$.

In the simulation, the Auger recombination coefficient and the recombination lifetime of the Shockley–Read–Hall were set to $2.0 \times 10^{-30} \text{ cm}^6 \text{ s}^{-1}$ and 100 ns.¹⁹ The built-in piezoelectric and spontaneous interface polarization charge densities were worked out based on the approach presented by Fiorentini *et al.*,^{20,21} assuming the screening factor for the polarization charges to be 0.25. In addition, the absorption coefficient (α) of each layer employs a linear function of the doping concentration using the formula¹⁸ $\alpha = \left(\frac{\text{doping}}{10^{19}} \times 50\right) \text{ cm}^{-1}$, where *doping* is the doping value of each layer in cm^{-3} . In addition, the indexes of refraction for AlN, GaN, and InN are set to 2.0767, 2.5067, and 3.4167, respectively, at around 410 nm laser wavelength in this work. Meanwhile, the indexes of refraction for AlGaIn and InGaIn are obtained by employing the linear interpolation method.²²

III. RESULTS AND DISCUSSIONS

Figure 1 indicates the simulated curves of laser power vs current (P - I) and current vs voltage (I - V) of the three LDs. The I - V curves clearly show that the turn-on voltage and the resistance of the LD with the IGI QBs are somewhat bigger than the counterparts of the LD with InGaN QBs and GaN QBs because of the extra interface barriers between InGaN and GaN in the IGI QBs. From the P - I curves, it can be observed that the threshold current of the LD with IGI and InGaN QBs is lower than that of the LD

with GaN QBs. Meanwhile, the LD with IGI QBs has the biggest output power of about 109 mW at 120 mA, compared with the LD with InGaN (about 100 mW) and GaN QBs (about 60 mW). Consequently, the slope efficiency of the LD with IGI QBs increased sharply with an efficiency of about 1.30 W/A, while the efficiencies of the LDs with InGaN and GaN QBs are about 1.14 and 0.76 W/A. Therefore, among the three LDs, the LD with IGI QBs has the best performance.

Figure 2 displays the distribution of the optical field for the three LDs and the refractive index outline of the LD with GaN QBs. It can be clearly observed that the maximum optical intensity was seen in the MQW region due to the optical confinement provided by the refractive index difference between the MQW region, the GaN waveguide, and the AlGaIn CL. Additionally, because the refractive index of the InGaIn QB is bigger than the index of the GaN QB, the optical field full width at half maximum (FWHM) decreases significantly when InGaIn QBs are substituted for the GaN QBs. Moreover, the optical field distribution of the LD with IGI QBs is almost the same as that of the LD with InGaIn QBs because the overall In content in the QBs of these two LDs is identical. The smaller FWHM indicates compression of the optical field, which is the better suppressed leakage out of the MQWs. Therefore, the OCF is increased and the OAL is reduced. The OCFs are 1.27%, 1.28%, and 1.18%, and the OALs are 58.1, 58.0, and 58.9 cm^{-1} for the LDs with IGI, InGaIn, and GaN QBs, respectively.

Figure 3 shows the distributions of carrier concentration for the three LDs at 120 mA. It can be seen that the electron concentrations in the MQWs are nearly the same order of magnitude [Fig. 3(a)] for all three LDs. For the conventional LDs with GaN QBs, the electron concentration from the n-side to the p-side gradually increases in the three QBs, thus leading to significant electron leakage on the p-side. When employing InGaIn QBs, the electron concentration changes relatively little in the left QBs and right QBs

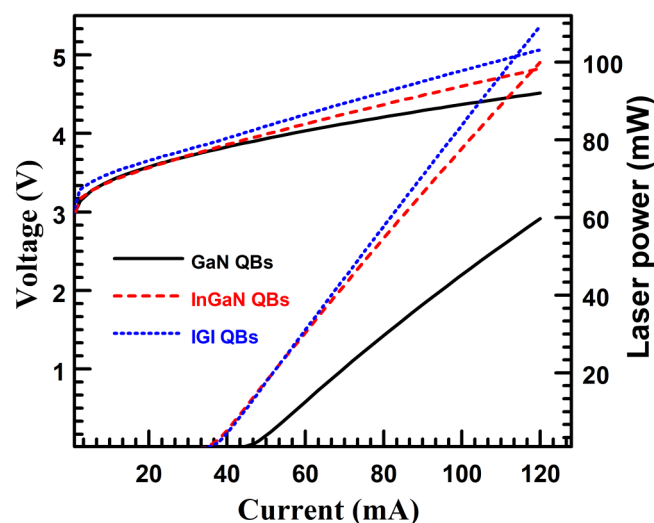


FIG. 1. The curves of laser power vs current (P - I) and current vs voltage (I - V) for the three LDs.

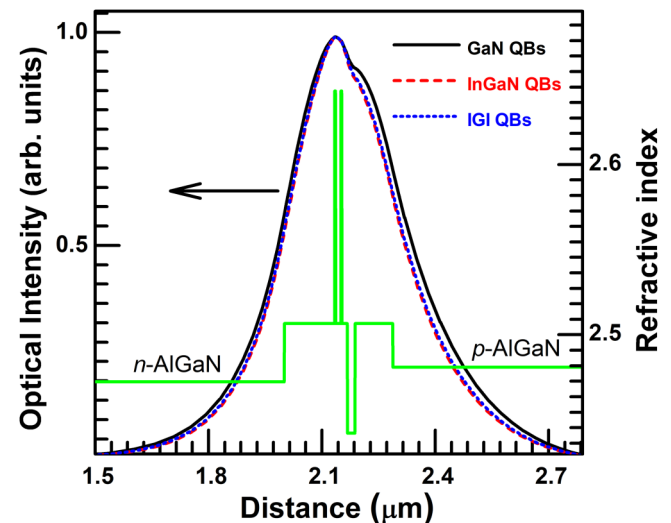


FIG. 2. The optical field distribution for the three LDs and the refractive index outline of the LD with GaN QBs.

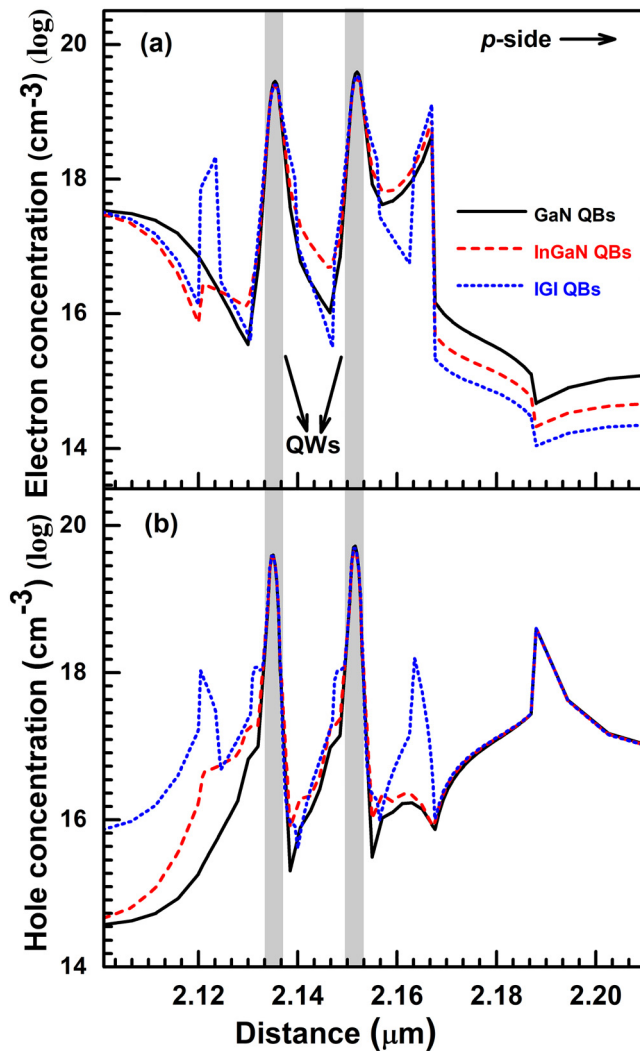


FIG. 3. (a) Electron concentrations and (b) hole concentrations of the three LDs at 120 mA. Gray regions are the locations of QWs.

compared with that in the LD with GaN QBs, but increases substantially in the middle QB, signifying that the leakage electron from the MQWs to the p-side is decreased. For the LD with IGI QBs, the electron concentration in the left QBs near the n-side increased over two orders of magnitude, whereas that in the right QB near the p-side decreased over one order of magnitude compared with the other two LDs. Therefore, electron leakage is substantially suppressed in the LD with IGI QBs as shown in Fig. 3(a). The hole concentrations in the MQWs for all three LDs are nearly the same order of magnitude [Fig. 3(b)], similar to the observations for the electron concentration distributions. However, when InGaN QBs are substituted for the GaN QBs, the hole concentration in the three QBs increases obviously, showing improved hole injection. Moreover, for the LDs with IGI QBs, most holes are confined to

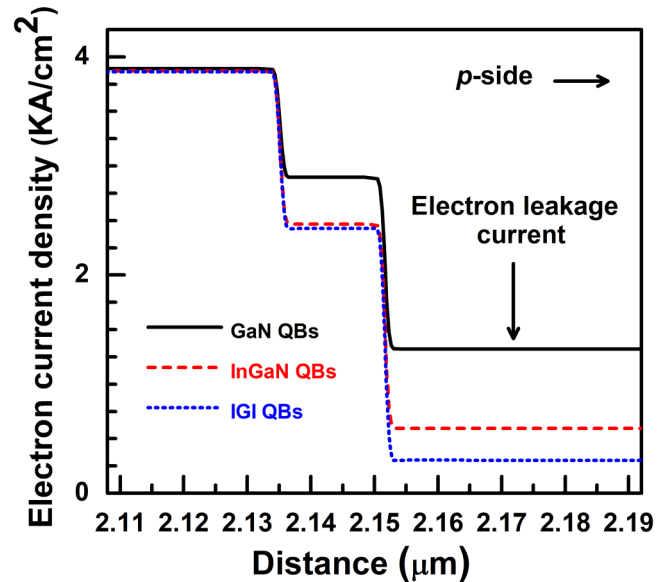


FIG. 4. The distributions of electron current density for the three LDs.

the interface of the n-waveguide/left QB as well as the interface of the right QB/EBL, which indicates that the suppression of electron leakage leads to increased ease of hole transport and enhanced efficiency of hole injection in this LD.

Figure 4 shows the simulated distributions of the electron current density for the three LDs. The electrons from the n-side are injected into the active region, then recombine in the MQW region

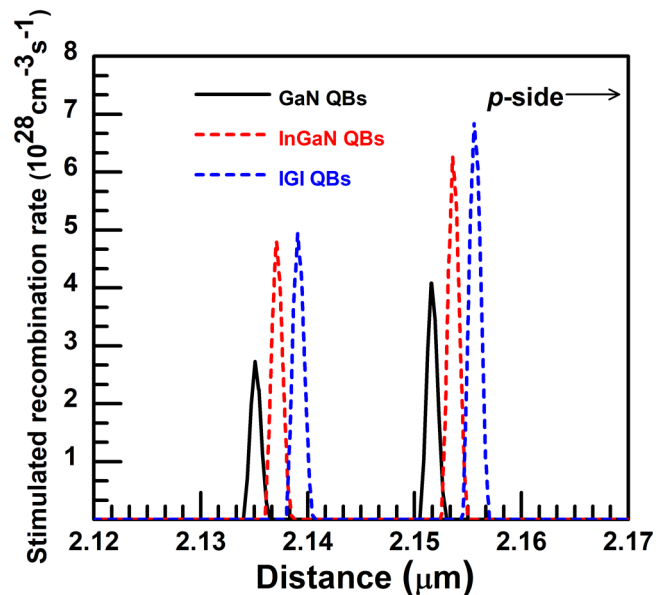


FIG. 5. The rates of stimulated recombination for the three LDs at 120 mA.

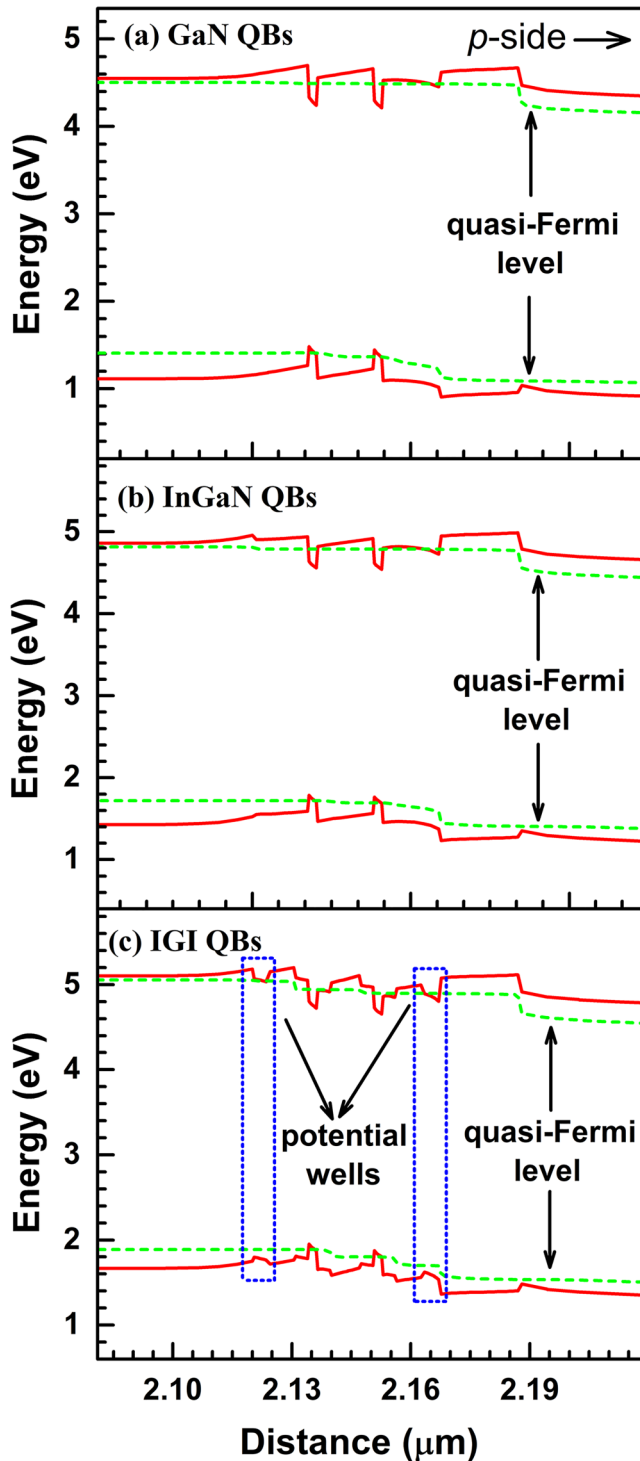


FIG. 6. Energy band diagrams of the LDs with (a) GaN QBs, (b) InGaN QBs, and (c) IGI QBs at 120 mA.

with holes, reducing current density through their transport directions. The electron current that leaks into the p-side is defined as the electron leakage current. For LDs with conventional GaN QBs, the leakage current density for electrons shows severe electron current leakage. When the InGaN QBs are substituted for the GaN QBs, the leakage current density for electrons is decreased and further decreased in the LD with IGI QBs.

Figure 5 shows the rates of stimulated recombination for the three LDs at 120 mA. For the LD with IGI QBs, more holes are injected into and more electrons are confined in the MQW region, as discussed above. In addition, the overlap of electrons and holes in the wave function increases in the LDs with IGI QBs because of the decrease in the polarization effect in the two QWs. Thus, the stimulated recombination rates in the LDs with IGI QBs are much larger than that in the LDs with InGaN and GaN QBs.

Figure 6 displays the energy band diagrams of the three LDs at 120 mA. For the LD with GaN QBs, the energy band shows serious bending mainly caused by the inherent polarization charge in the GaN-based LDs, which affects the effective potential barrier height of the QBs that confine the carriers in the QWs and of the EBL that impede electrons leaking into the p-side. When InGaN QBs are substituted for the GaN QBs, the improvement in the lattice constant match of the InGaN QWs and QBs alleviates the bending of the energy band in the QBs and QWs, which is useful for the transport and recombination of the carriers in the MQWs. Meanwhile, in the electron conduction band, the EBL's effective potential barrier height is increased because the energy bandgap difference in the AlGaIn EBL and the last InGaIn QB is larger than the counterpart of the AlGaIn EBL and the last GaN QB. With the higher EBL's effective potential barrier height, the leakage electron could be more efficiently suppressed. When using the IGI QBs, the EBL's effective potential barrier for electrons is further increased because the In content in the IGI QBs is higher than that in the InGaIn QBs. In addition, inserting the GaN layer into the InGaIn QB can increase the potential barrier of the QB for carrier confinement in the QWs. These are the causes of the superior suppression of electron leakage in the LD with IGI QBs. Furthermore, two potential wells are formed in the energy band: one potential well lies in the first QB near the n-GaN waveguide; another lies in the last QB near the AlGaIn EBL. Therefore, most injected carriers can accumulate in these two potential wells. Moreover, for the LD with IGI QBs, the valence band energy of the right potential well for holes near the p-side is significantly lower than its counterpart of the p-GaN waveguide and higher than that of the QWs. The resultant ease of tunneling of the holes in the p-side into the MQWs though this potential well is useful for improvement of hole injection.

IV. SUMMARY

In conclusion, we have numerically studied the characteristics of the InGaIn LDs with InGaIn, GaN, and IGI QBs. Our results show that the LD with IGI QBs exhibits the best optical and electrical performance among the three LDs because it has the highest output power, the lowest threshold current, and the greatest slope efficiency. The main physical cause for the improvement of these properties is presumably the proper adjustment of the refraction

index profile and energy band diagrams, which are advantageous to the suppressed leakage of the optical field and electrons out of and the enhanced injection of holes into the MQWs.

ACKNOWLEDGMENTS

The authors acknowledge the support from the Key Research & Development Program of Jiangsu Province under Grant Nos. BE2020083 and BE2020083-4, Equipment Pre-Research Program under Grant No. 2006ZYGG0304, and Science and Technology Program of Yangzhou under Grant No. YZ2020024.

AUTHOR DECLARATIONS

Conflict of Interest

The authors have no conflicts to disclose.

DATA AVAILABILITY

The data that support the findings of this study are available from the corresponding author upon reasonable request.

REFERENCES

- ¹H. Fu, W. Sun, O. Ogidi-Ekoko, J. C. Goodrich, and N. Tansu, *AIP Adv.* **9**, 045013 (2019).
- ²T.-C. Wu, Y.-C. Chi, H.-Y. Wang, C.-T. Tsai, C.-H. Cheng, J.-K. Chang, L.-Y. Chen, W.-H. Cheng, and G.-R. Lin, *J. Lightwave Technol.* **36**, 1634–1643 (2018).
- ³A. A. Bergh, *Phys. Status Solidi A* **201**, 2740 (2004).
- ⁴J. Yang, Z. Liu, B. Xe, Z. Liao, L. S. Feng, N. Zhang, J. X. Wang, and J. M. Li, *IEEE Photonics J.* **10**, 8200508 (2018).
- ⁵J. J. Wierer, J. Y. Tsao, and D. S. Sizov, *Laser Photonics Rev.* **7**, 963–993 (2013).
- ⁶K. Orita, M. Meneghini, H. Ohno, N. Trivellin, N. Ikeda, S. Takigawa, M. Yuri, T. Tanaka, E. Zanoni, and G. Meneghesso, *IEEE J. Quantum Electron.* **48**, 1169–1176 (2012).
- ⁷G. Alahyarizadeh, M. Amirhoseiny, and Z. Hassan, *Opt. Laser Technol.* **76**, 106–112 (2016).
- ⁸W. Yang, D. Li, N. Liu, Z. Chen, L. Wang, L. Liu, L. Li, C. Wan, W. Chen, X. Hu, and W. Du, *Appl. Phys. Lett.* **100**, 031105 (2012).
- ⁹M. Zhou, F. Liang, and D. G. Zhao, *J. Mater. Sci.: Mater. Electron.* **31**, 5814–5819 (2020).
- ¹⁰C. Netzel, V. Hoffmann, S. Einfeldt, and M. Weyers, *J. Electron. Mater.* **49**, 5138–5143 (2020).
- ¹¹A. Stolz, E. Cho, E. Dogheche, Y. Androussi, D. Troadec, D. Pavlidis, and D. Decoster, *Appl. Phys. Lett.* **98**, 161903 (2011).
- ¹²M.-X. Feng, J.-P. Liu, S.-M. Zhang, D.-S. Jiang, Z.-C. Li, D.-Y. Li, L.-Q. Zhang, F. Wang, H. Wang, and H. Yang, *IEEE J. Sel. Top. Quantum Electron.* **19**, 1500705 (2013).
- ¹³R. M. Farrell, D. A. Haeger, P. S. Hsu, M. C. Schmidt, K. Fujito, D. F. Feezell, S. P. DenBaars, J. S. Speck, and S. Nakamura, *Appl. Phys. Lett.* **99**, 171113 (2011).
- ¹⁴A. Paliwal, K. Singh, and M. Mathew, *Semicond. Sci. Technol.* **35**, 045022 (2020).
- ¹⁵B. Cheng, C. L. Chua, Z. Yang, M. Teepe, C. Knollenberg, A. Strittmatter, and N. Johnson, *IEEE Photonics Technol. Lett.* **22**, 329–331 (2010).
- ¹⁶J. Yang, D. G. Zhao, Z. S. Liu, D. S. Jiang, J. J. Zhu, P. Chen, F. Liang, S. T. Liu, W. Liu, Y. Xing, and M. Li, *IEEE Photonics J.* **10**, 1503107 (2018).
- ¹⁷LASTIP by Crosslight Software Inc., Burnaby, Canada, see <http://www.crosslight.com>.
- ¹⁸F. Liang, D.-G. Zhao, D.-S. Jiang, Z.-S. Liu, J.-J. Zhu, P. Chen, J. Yang, W. Liu, S.-T. Liu, Y. Xing, L.-Q. Zhang, W.-J. Wang, M. Li, Y.-T. Zhang, and G.-T. Du, *Jpn. J. Appl. Phys.* **57**, 070307 (2018).
- ¹⁹Y. C. Shen, G. O. Mueller, S. Watanabe, N. F. Gardner, A. Munkholm, and M. R. Krames, *Appl. Phys. Lett.* **91**, 141101 (2007).
- ²⁰V. Fiorentini, F. Bernardini, and O. Ambacher, *Appl. Phys. Lett.* **80**, 1204–1206 (2002).
- ²¹Y. Chen, Y. Wang, Z. Wang, Y. Gu, Y. Ye, X. Chai, J. Ye, Y. Chen, R. Xie, Y. Zhou, Z. Hu, Q. Li, L. Zhang, F. Wang, P. Wang, J. Miao, J. Wang, X. Chen, W. Lu, P. Zhou, and W. Hu, *Nat. Electron.* **4**, 357–363 (2021).
- ²²P. Chen, D. G. Zhao, D. S. Jiang, J. J. Zhu, Z. S. Liu, J. Yang, X. Li, L. C. Le, X. G. He, W. Liu, X. J. Li, F. Liang, B. S. Zhang, H. Yang, Y. T. Zhang, and G. T. Du, *AIP Adv.* **6**, 035124 (2016).